

Masahiko Demura,<sup>1</sup> Kyosuke Kishida,<sup>1</sup> Osamu Umezawa,<sup>1</sup> Easo P. George,<sup>2</sup> and Toshiyuki Hirano<sup>1</sup>

## Ductile Thin Foils of Ni<sub>3</sub>Al

---

**REFERENCE:** Demura, M., Kishida, K., Umezawa, O., George, E. P., and Hirano, T., "Ductile Thin Foils of Ni<sub>3</sub>Al," *Mechanical Properties of Structural Films, STP 1413*, C. Muhlstein and S. B. Brown, Eds., American Society for Testing and Materials, West Conshohocken, PA, Online, Available: [www.astm.org/STP/1413/1413\\_04](http://www.astm.org/STP/1413/1413_04), 16 March 2001.

**ABSTRACT:** Ni<sub>3</sub>Al thin foils with 315 to 357 μm thickness were successfully fabricated by cold rolling. X-ray pole figures showed the formation of {110} rolling textures with various rolling directions in the foils cold rolled over 83% reduction. The deformation microstructure consists of fine slip traces and coarse and wavy shear bands. Banded deformation structure was observed in some foils. In the foils cold rolled to 83% reduction, the Vickers hardness number reached over 600 and the ultimate tensile strength over 1.7 GPa, irrespective of rolling texture and deformation microstructure. The cold rolled foils showed no tensile elongation, but it was possible to bend the foils. The foils recrystallized at temperatures over 1273 K had some tensile ductility (3.0 to 14.6%), though the polycrystalline Ni<sub>3</sub>Al is known to be brittle due to severe grain boundary fracture. Electron backscatter diffraction measurements revealed that the large amount of total grain boundary area consists of low angle (LAB) and Σ3 coincidence lattice boundaries. This large fraction is probably a chief cause of the observed ductility.

**KEYWORDS:** intermetallic compounds, Ni<sub>3</sub>Al, foil, cold rolling, texture, microstructure, mechanical properties, recrystallization, ductility

### Introduction

Heat-resistant metallic foils have become important structural materials in microelectromechanical systems (MEMS) such as power-producing devices and chemical reactors [1]. Metallic foils have the advantage of high fracture toughness over ceramics, silicon carbides, alumina, et al. In semiconductor devices, Wagner and his co-workers [2-4] have recently fabricated silicon-based thin-film transistors on stainless steel foils with thickness ranging from 25 to 200 μm in order to provide flexibility and durability.

At present metallic foils below 100 μm in thickness are limited to ductile common metals, for example, aluminum, nickel, and stainless steel. Unfortunately, the high-temperature strength of these metals is low, and corrosion and oxidation resistances are not good enough. Compared to these common metals, intermetallic compounds have excellent physical and/or mechanical properties. In particular, Ni<sub>3</sub>Al, whose crystal structure is of ordered fcc, L1<sub>2</sub>, has attractive high-temperature properties such as anomalous strengthening with increasing temperature (see Fig. 1 [5,6]) and excellent resistance to oxidation and corrosion (see the review by Stoloff [7]). Table 1 lists the other physical properties at room temperature. Compared with stainless steel [6], Ni<sub>3</sub>Al has higher thermal conductivity, lower coefficient of thermal expansion, and lower electrical resistivity, while the density and elastic constant are comparable. Because of

---

<sup>1</sup> National Research Institute for Metals, Sengen 1-2-1, Tsukuba, Ibaraki 305-0047, Japan.

<sup>2</sup> Oak Ridge National Laboratory, Oak Ridge, TN 37831-6093.

these excellent properties,  $\text{Ni}_3\text{Al}$  is considered to be a promising material for MEMS.

However, thin foils, particularly by cold rolling, have been unrealistic in brittle intermetallic compounds. In the case of  $\text{Ni}_3\text{Al}$ , the brittleness arises from intergranular fracture [9]. It is well known that the brittleness can be overcome by micro-alloying with boron additions [10,11], but with all this beneficial effect, the ductility is not sufficient to fabricate thin foils on an engineering scale by cold rolling [12]. Alternatively, we previously found that the directional solidification (DS) using a floating zone (FZ) method provides a significant ductility improvement for  $\text{Ni}_3\text{Al}$  without any alloying elements [13,14]. DS materials show high tensile elongation at room temperature in ambient air, more than 70%, even though they are of polycrystalline form with columnar-grained structure [15]. This ductility is larger than that of the boron-doped alloy, 53.8%, reported by Liu et al. [11]. The high ductility of the DS polycrystals was ascribed to the large fraction of low angle and low  $\Sigma$ -value coincidence site lattice boundaries in the columnar-grained structure [16]. Using this technique we recently have succeeded in growing single crystals of stoichiometric  $\text{Ni}_3\text{Al}$  [17,18], which has previously been considered to be difficult. As is well known, monocrystalline  $\text{Ni}_3\text{Al}$  has substantial ductility, more than 100% elongation [9]. Taking advantage of the high ductility of these DS materials, we have fabricated thin foils with thickness ranging from 53 to 300  $\mu\text{m}$  by cold rolling [19].

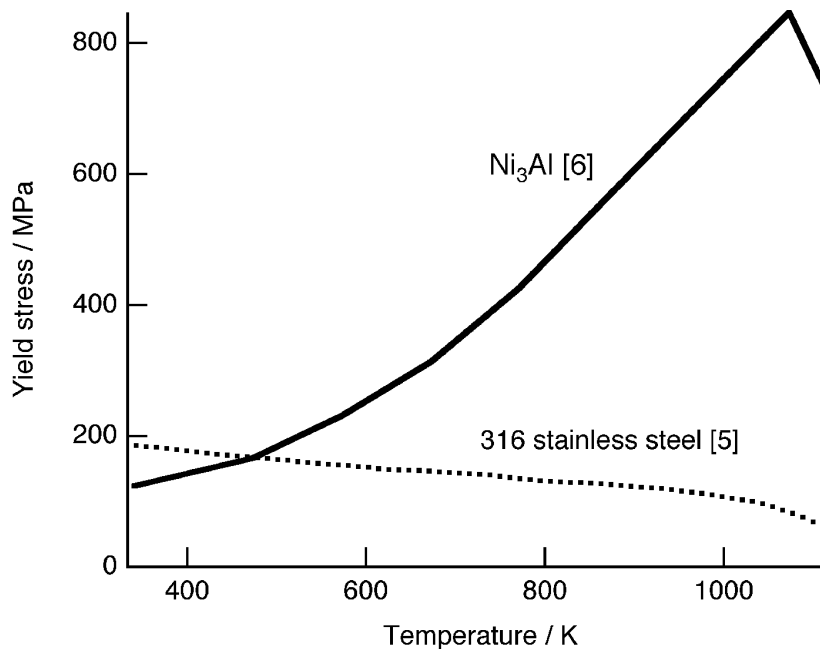


FIG. 1—Temperature dependence of yield stress of  $\text{Ni}_3\text{Al}$  single crystal with  $\langle 100 \rangle$  tensile direction, compared with those of 316 stainless steel.

TABLE 1—Density, elastic constant, thermal conductivity, coefficient of thermal expansion, and electrical resistivity of  $Ni_3Al$ , compared with common metallic alloys such as 316 stainless steel, Al, and Ni at room temperature.

Material	Density ( $g\ cm^{-3}$ )	Young's Modulus (GPa)	Thermal Conductivity ( $W\ m^{-1}\ K^{-1}$ )	Coefficient of Thermal Expansion ( $10^{-6}\ K^{-1}$ )	Electrical Resistivity ( $\mu\ \Omega\ cm$ )
$Ni_3Al$	7.5	180	29	12.5	33
316 stainless steel	7.9	190	17	17	72
Al	2.7	70	238	24	2.7
Ni	8.9	200	88	13	6.9

The purpose of this paper is to present the deformation microstructure, rolling texture, and basic mechanical properties of the cold rolled foils. Another purpose is to examine the ductility of recrystallized foils in air at room temperature. This is because loss of ductility due to recrystallization is of great concern for structural applications. Cold-worked  $Ni_3Al$  recrystallizes at high temperatures and forms equiaxed grains which are similar to those in the cast and homogenized alloys. As is well known, these alloys are very brittle in the absence of boron [9,11]. They fracture at grain boundaries just after yielding mostly due to the presence of moisture in air [20,21]. Thus, we present here the recrystallized microstructures of the foils and the room-temperature tensile properties in air.

TABLE 2—Analyzed Al contents and initial orientation (rolling plane and direction).

Sample No.	Al Content (at%)	Initial Orientation	
		Rolling Plane	Rolling Direction
31-2	24.4	{0.2 0.1 1.0}	<1.0 0.0 0.2>
41-1	24.7	{3.9 1.0 5.2}	<4.0 9.0 4.8>
42-2	24.8	{2.0 1.0 4.3}	<1.1 2.0 1.0>
47-1	24.6	{3.0 0.1 4.9}	<0.0 1.0 0.0>

### Experimental Procedures

Four rods, designated as Nos. 31-2, 41-1, 42-2, and 47-1 of boron-free binary stoichiometric Ni<sub>3</sub>Al, were grown by the FZ method in an image furnace with double halogen lamps at a growth rate of 25 mm/h. The feed rod preparation and crystal growth procedure were previously described [13]. In order to obtain high single crystallinity, the crystal diameter was kept constant during the crystal growth by controlling the power of the lamps. On average the grown rods were 12 mm in diameter and 150 mm in length. Table 2 summarizes the Al contents of the four rods as determined by inductively coupled plasma spectroscopy. The Al contents are close to the stoichiometric composition (25 at% Al).

The grown rods were sectioned into sheets along the growth direction by electric discharge machining (EDM). Their surfaces were mechanically polished. The optical microstructures were examined by etching with marble reagent (2.5 g CuSO<sub>4</sub>, 30 cm<sup>3</sup> HCl, and 25 cm<sup>3</sup> H<sub>2</sub>O). Samples Nos. 31-2 and 47-1 were mostly single crystal but contained columnar grains with low angle boundaries in places. Samples Nos. 41-1 and 42-2 were single crystals. The initial rolling direction (or growth direction) and rolling plane of the sheets were determined by the Laue X-ray back reflection method as summarized in Table 2.

The sheets (about 1 or 2 mm in initial thickness, see Table 3) were cold-rolled to about 300 μm in thickness by using four-high mills with a work roll diameter of 110 mm (10% reduction per pass). Then, they were rolled further using cemented carbide rolls having a roll diameter of 75 mm (2% reduction per pass). Both the cold-rolling operations were performed without intermediate annealing or lubricant.

The rolling textures of the foils were measured by X-ray Schultz back reflection method. Optical microscopic examination, after polishing with Al<sub>2</sub>O<sub>3</sub> paste and etching with the marble reagent, was conducted on the surface and the longitudinal section of the cold rolled foils. Basic mechanical properties of the cold rolled foils were examined by using samples Nos. 42-2 and 47-1. Vickers hardness was measured along the thickness direction on the longitudinal section. Tensile specimens with a gage length of 10 mm and a width of 5 mm were cut by EDM. Tensile tests were performed at room temperature in air at a strain-rate of  $8 \times 10^{-4} \text{ s}^{-1}$ . The load data were collected at a frequency of 5 Hz with a computer.

The tensile properties of the recrystallized foils were studied using two foils of sample No. 31-2 with two different thicknesses: 73 μm—thick foil (92% reduction) and 315 μm—thick foil (67% reduction). These foils were recrystallized at 1273 K and 1573 K for 1.8 ks in a vacuum better than  $1 \times 10^{-4}$  Pa. The optical microstructures were examined by etching with Marble reagent. The average grain size was measured by line intercept method without correction. The orientation of the recrystallized grains was measured at 1 or 5 μm scanning steps by electron back scatter diffraction (EBSD) in a scanning electron microscope (SEM).

The grain boundary (GB) character, or Σ-value, was calculated based on Brandon's criterion [22]: if the deviation angle from an exact coincidence site lattice (CSL) relation is less than  $15^\circ/\Sigma^{1/2}$ , the boundary is referred to as a CSL boundary with that Σ-value. The maximum Σ-value was set as 25 (i.e., those with higher Σ-values were

designated as random boundaries). The area fraction of each GB type was two-dimensionally evaluated by measuring GB length in the EBSD-SEM image, instead of number fraction.

Tensile specimens with gage length of 10 mm were cut from the recrystallized foils by electric discharge machining. The gage widths were 3 mm and 5 mm for 73  $\mu\text{m}$  and 315  $\mu\text{m}$  thick foils, respectively. Tensile tests were performed at room temperature in air at a strain-rate of  $8 \times 10^{-4} \text{ s}^{-1}$  in the same way as those for cold rolled foils. The fracture surface was examined by SEM.

## Results and Discussion

### *Cold Rolled Foils*

It was possible to cold-roll the starting sheets to thin foil less than 100  $\mu\text{m}$  in thickness without intermediate annealing. Figure 2 shows a 1 m long foil of sample No. 41-1 that is 91  $\mu\text{m}$  thick and 10 mm wide. In this case the total reduction in thickness amounts to 96%. The surface is crack-free and smooth with little fluctuation in thickness (less than 1  $\mu\text{m}$ ) along the rolling direction. With a shiny metallic luster it looks like a mirror. It is worth noting that such high-quality thin foil was fabricated by cold rolling boron-free, binary  $\text{Ni}_3\text{Al}$ , which is considered a brittle intermetallic compound.

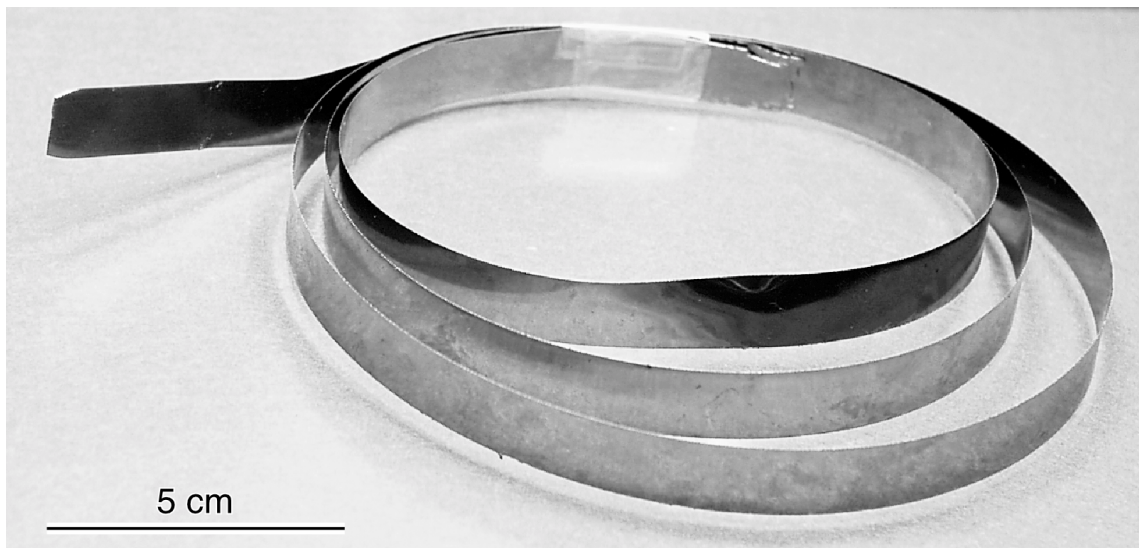


FIG. 2—91  $\mu\text{m}$  thick, 10 mm wide and about 1 m long foil of sample No. 41-1 cold-rolled to 96% reduction in thickness.

TABLE 3— *Results of cold rolling: thickness of the sheet before and after cold rolling, reduction in thickness, and rolling texture.*

Sample No.	Thickness / $\mu\text{m}$		Reduction (%)	Rolling Texture
	Before Rolling	After Rolling		
31-2	959	315	67	... <sup>a</sup>
		73	92	{110}<113> + {110}<117>
		57	94	... <sup>a</sup>
41-1	2043	91	96	{110}<113>
42-2	1907	319	83	{110}<113>
47-1	1789	302	83	Diffused {110}<117>

<sup>a</sup>Not measured.

Similarly high rolling ductility was obtained in other samples, Nos. 31-2, 42-2, and 47-1, which had different initial orientations (Table 2). The results are summarized in Table 3. Samples Nos. 41-1 and 42-2 are single crystals, and hence the results may be somewhat expected because  $\text{Ni}_3\text{Al}$  is known to be ductile in a single crystal form [9]. In the case of binary, stoichiometric alloys, the problem is the difficulty in growing single crystal [18]. Samples Nos. 31-2 and 47-1 had some columnar grains, but this did not hinder cold rolling. As we previously reported [14], the columnar-grained polycrystals grown by the FZ method are ductile because most of the boundaries are low-angle and low  $\Sigma$  types [16].

Figure 3 shows two typical types of deformation microstructures observed in cold rolled foils. Slip traces appear on the surface and the longitudinal section after chemical etching. In the foil of Sample No. 42-2 (83.4% reduction), fine slip traces lie on the surface, being inclined about  $60^\circ$  to the rolling direction. Also, coarse and wavy lines, which are regarded as shear bands [23], are observed clearly on the longitudinal section, indicating inhomogeneous plastic deformation. These deformation microstructures, i.e., fine slip traces and wavy shear bands, are common in all the foils cold rolled over 83%. In the case of samples Nos. 47-1 (83.1% reduction) and 31-2 (92% reduction), however, the deformation structure is composed of repeated two bands with differently oriented slip lines. The width of the bands ranges from 20 to 100  $\mu\text{m}$  parallel to the rolling direction [Fig. 3(b)].

Figure 4 shows the {220} pole figures of the foils cold rolled to 83% reduction: (a) sample No. 42-2 and (b) No. 47-1. In all the foils cold rolled over 83% reduction, the

{220} pole has the highest intensity peak at the normal direction (ND) and surrounding high intensity regions about 60 degrees away from the ND. This shows that the surface is almost parallel to {110} plane. This {110} texture is thought to be stable in Ni<sub>3</sub>Al under compressive deformation normal to the rolling plane, as discussed elsewhere [19]. Regarding the rolling direction (RD), there is some difference among the samples, as seen in Table 3. Samples Nos. 41-1 and 42-2 possess a single {110}<113> texture. On the other hands, sample No. 31-2 consists of {110}<113> and {110}<117> textures. Sample No. 47-1 has a {110} texture, but the RD scatters around <117> direction, which indicates that the {110} texture consists of grains with slightly different RD. Probably the difference observed in the texture is due to the initial orientation of the sheet.

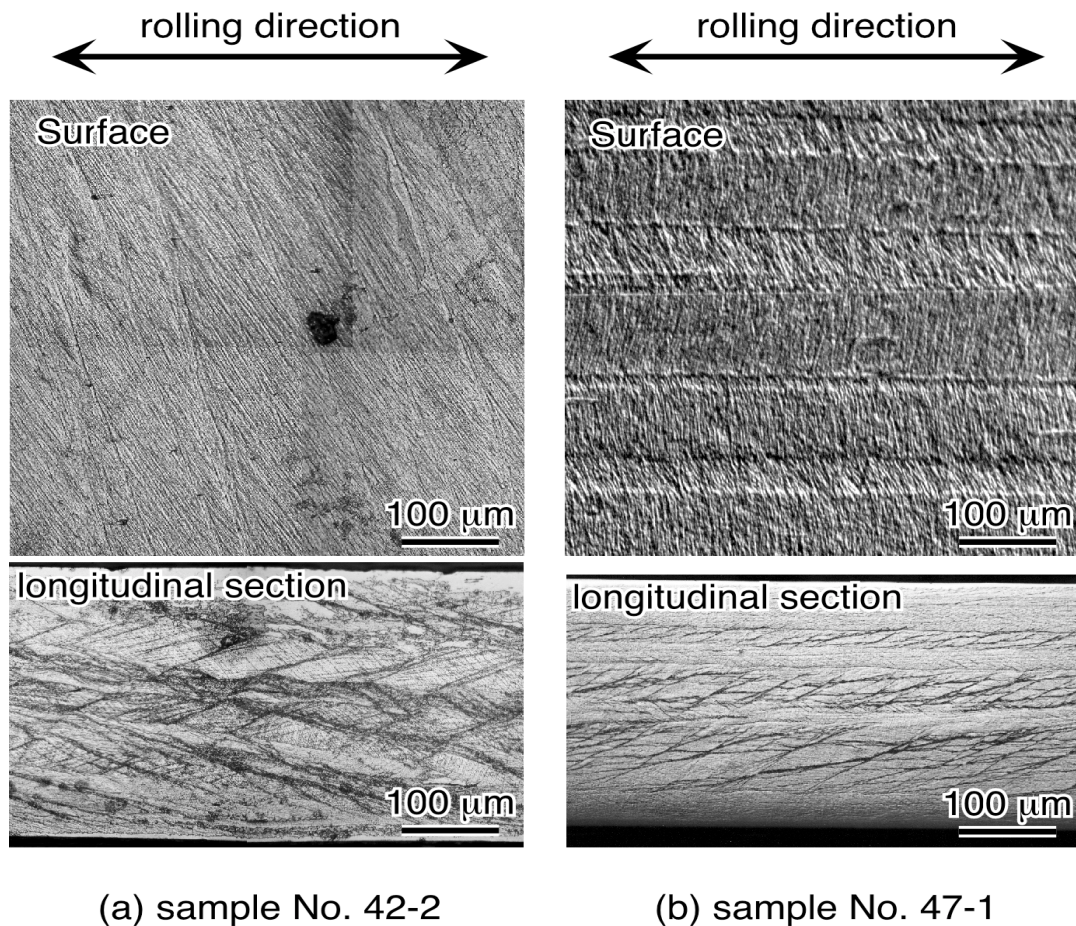


FIG. 3—Optical microstructures observed on the etched surface and longitudinal section of cold rolled foils: (a) sample No. 42-2 and (b) No. 47-1.

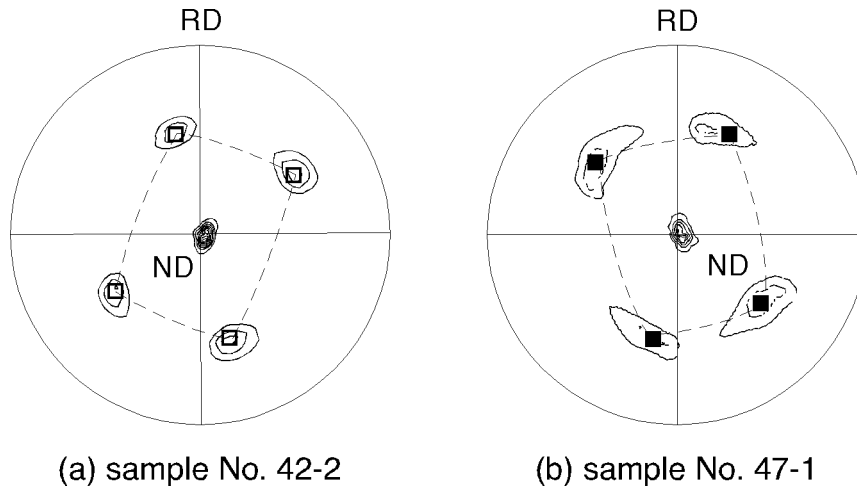


FIG. 4—The  $\{220\}$  pole figures of the foils cold rolled to 83% reduction: (a) sample No. 42-2 and (b) No. 47-1. Open and solid squares represent  $\{110\}\langle 113\rangle$  and  $\{110\}\langle 117\rangle$  textures, respectively.

Mechanical properties were examined by using the foils of samples Nos. 42-2 and 47-1, which were cold rolled to almost the same reduction, 83%. In both the foils, there was no appreciable change in the hardness number along the thickness direction. This indicates that macroscopically the foils are homogeneously cold-rolled. Average Vickers hardness numbers are 604 for sample No. 42-2 and 649 for No. 47-1, showing no significant difference. For reference, the Vickers hardness number of the starting sheet before cold rolling was about 260.

Figure 5 plots the engineering stress vs. engineering strain curves for samples Nos. 42-2 and 47-1. Since the foils are heavily cold rolled, they show extremely high tensile strengths: 1.7 GPa for sample No. 42-2 and 1.9 GPa for sample No. 47-1. Both the foils fractured with almost no plastic elongation. In spite of such brittle behavior, interestingly it is possible to bend as shown in Fig. 6, probably because of the thinness of the foils. There is almost no difference in the tensile properties and the Vickers hardness number between the two samples, though their deformation microstructures and textures are different.

#### *Recrystallized Foils*

It has been reported that the recrystallization of  $\text{Ni}_3\text{Al}$  starts between 900 and 1000 K, depending on the amount of rolling reduction [24]. Consistent with this, both 73  $\mu\text{m}$  and 315  $\mu\text{m}$  thick foils of sample No. 31-2 were fully recrystallized above 1273 K. Figure 7 is an optical micrograph of the 73  $\mu\text{m}$  thick foil heat-treated at 1273 K for 1.8 ks. It shows a typical recrystallized microstructure that consists of equiaxed grains with homogeneous grain size. A similar grain morphology was observed in the foils heat-treated above 1273 K and also in the 315  $\mu\text{m}$  thick foils. Table 4 lists the average grain sizes of 73  $\mu\text{m}$  and 315  $\mu\text{m}$  thick foils recrystallized at 1273 K and 1573 K. The grain size increases with increasing heat treatment temperature, as expected.



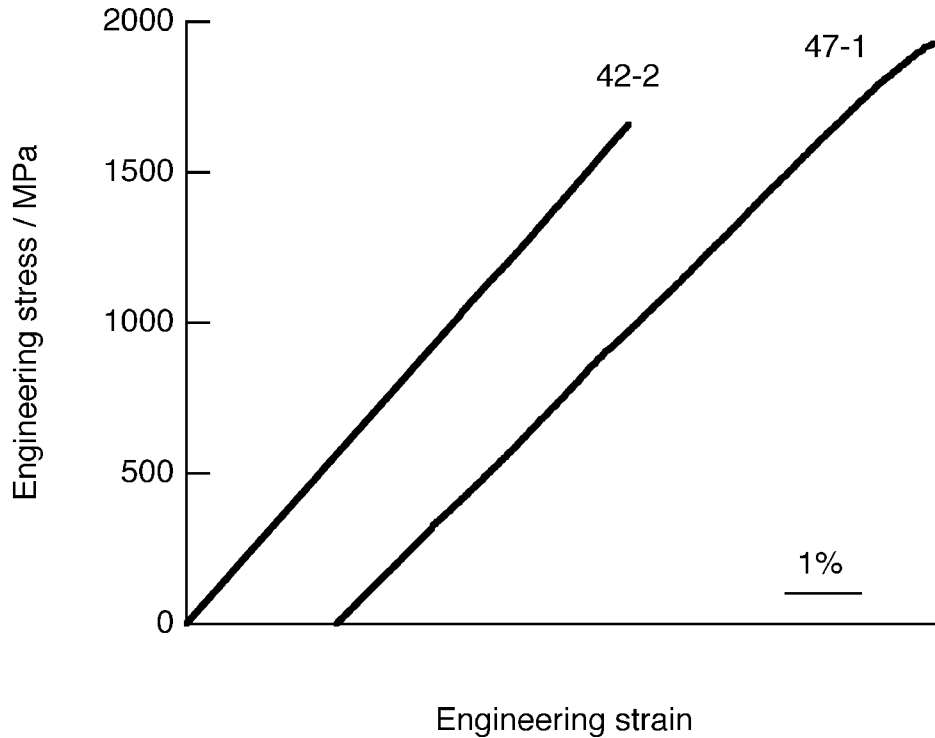


FIG. 5—Engineering stress vs. engineering strain curves of the foils cold rolled to 83% reduction of samples Nos. 42-2 and 47-1.

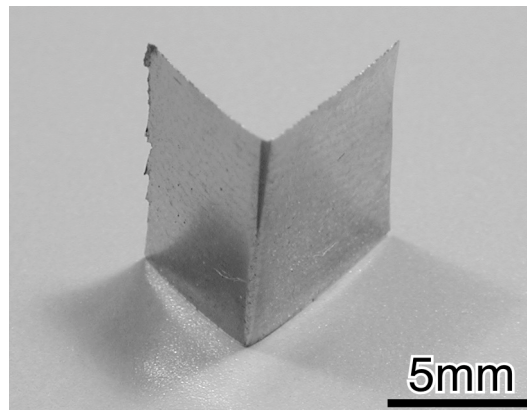


FIG. 6—Photograph of 91  $\mu\text{m}$ -thick foil cold rolled to 96% reduction of sample No. 41-1, showing bending.

Table 4 summarizes the area fraction of each GB type in the 73  $\mu\text{m}$  and 315  $\mu\text{m}$  thick foils of sample No. 31-2 recrystallized at 1273 K and 1573 K. The recrystallized foils consist mostly of three types of boundaries, low angle (LAB),  $\Sigma 3$ , and random boundaries (RB). Very small amounts of CSL boundaries between  $\Sigma 5$  and 25 exist in the foils recrystallized at 1273 K. Note that the foils have a large fraction of LAB and  $\Sigma$

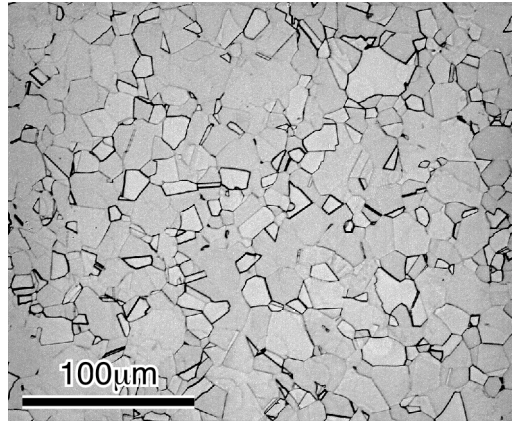


FIG. 7—Microstructure of 73  $\mu\text{m}$ -thick foil of sample No. 31-2 recrystallized at 1273 K for 1.8 ks.

boundaries, which are considered to be crack-resistant [25,26]. There is a tendency that as the heat treatment temperature increases, the total fraction of LAB and  $\Sigma 3$  increases, and the fraction of RB, which is considered to be very susceptible to cracking, decreased.

Tensile properties, i.e., yield stress and elongation to fracture, of 73  $\mu\text{m}$  and 315  $\mu\text{m}$  thick foils of sample No. 31-2 recrystallized at 1273 K and 1573 K are summarized in

TABLE 4—Average grain size, area fraction of grain boundary types, and tensile properties, yield stress (YS) and fracture elongation (FE) in the recrystallized foils of No. 31-2.

Thickness ( $\mu\text{m}$ )	Heat Treatment Temperature (K)	Average Grain Size ( $\mu\text{m}$ )	Area Fraction (%)				Tensile Properties	
			LAB	$\Sigma 3$	$\Sigma 5-25$	RB	YS (MPa)	FE (%)
73	1273	11.9	11.7	31.0	3.1	54.2	250	3.0
73	1573	66.9	44.3	15.6	0.0	40.1	50	5.6
315	1273	14.5	3.2	37.8	0.8	58.2	294	3.4
315	1573	115	73.2	10.8	0.0	16.0	70	14.2

Table 4. Note that all the foils show some ductility after yielding. In particular, the foils recrystallized at 1573 K, which show 5.6% and 14% elongations for 73  $\mu\text{m}$  and 315  $\mu\text{m}$  thick foils, respectively. Though the ductility decreases with decreasing recrystallization temperature, the foils recrystallized at 1273 K still show 3% elongation. Thus, the ductility loss due to recrystallization is not a serious problem in our foils. These ductilities normally cannot be expected for boron-free polycrystalline  $\text{Ni}_3\text{Al}$ . The yield stress decreases with increasing recrystallization temperature, because of the increase in grain size.

Figure 8 shows the fracture surfaces of the recrystallized foils after the above tensile tests. Intergranular fracture is dominant in both the 73  $\mu\text{m}$  and 315  $\mu\text{m}$  thick foils recrystallized at 1273 K, while the fraction of transgranular fracture is rather high in the foils recrystallized at 1573 K. The change in fracture mode correlates well with both the ductility and the fraction of the LAB and  $\Sigma 3$  boundaries (Table 4). It is, therefore,

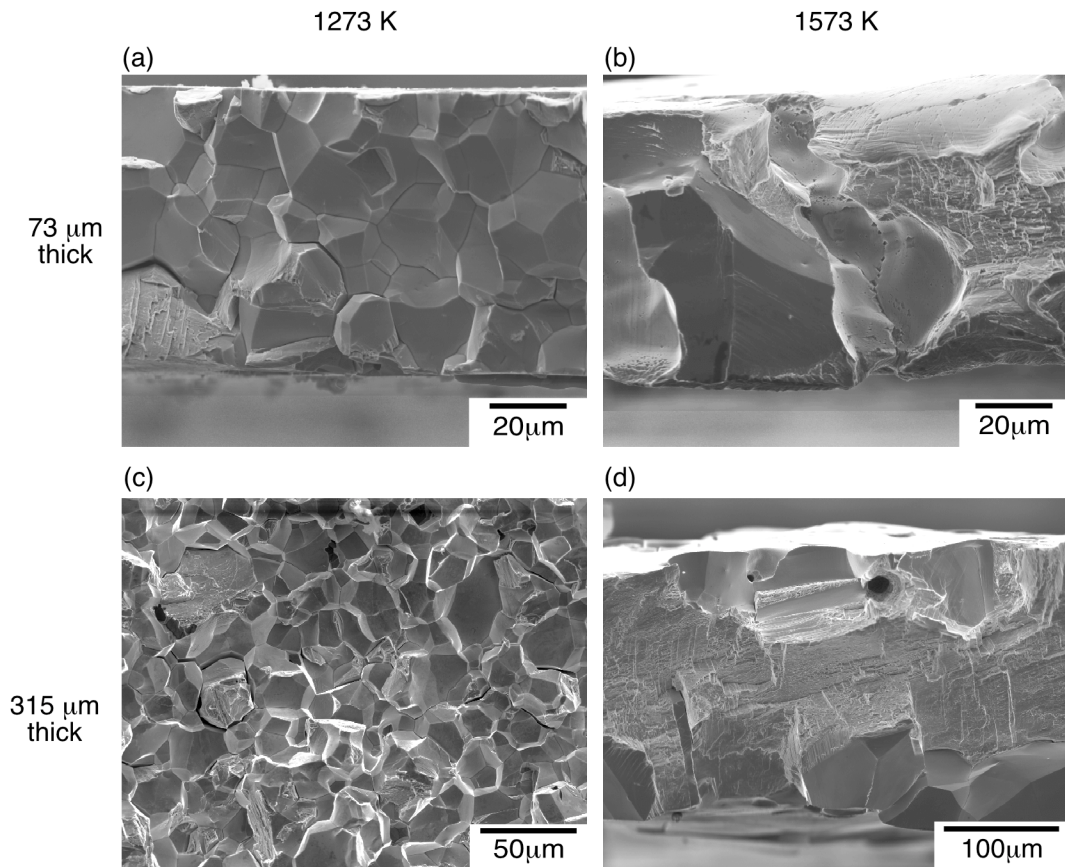


FIG. 8—Fracture surfaces of the recrystallized foils of sample No. 31-2: (a) 73  $\mu\text{m}$ -thick foil recrystallized at 1273 K, (b) 73  $\mu\text{m}$ -thick at 1573 K, (c) 315  $\mu\text{m}$ -thick at 1273 K, and (d) 315  $\mu\text{m}$ -thick at 1573 K.

concluded that with increasing heat treatment temperature, the fraction of the crack-resistant boundaries, LAB and  $\Sigma 3$ , increases, resulting in high ductility by suppressing intergranular fracture.

Probably, the ductility of recrystallized foils is mainly due to the high area fraction of LAB and  $\Sigma 3$  boundaries. Hanada et al. [25] found no cracks along these boundaries in bent specimens of recrystallized, stoichiometric  $\text{Ni}_3\text{Al}$ , suggesting higher crack-resistance compared to other boundaries. This was confirmed by Lin and Pope [26] who examined the distribution of cracked boundaries as a function of  $\Sigma$ -value in bent specimens of melt-spun  $\text{Ni}_3(\text{Al}, 0.2\text{at}\% \text{Ta})$  ribbons. In addition to these qualitative evaluations of grain boundary fracture strength, very recently we found that these LAB and  $\Sigma 3$  boundaries do not fracture in air by performing uniaxial tensile tests on bicrystal specimens, instead the bulk fractures [27]. This new finding shows that the fracture strength of these two types of boundaries is at least comparable to that of the bulk, which confirms that the presence of these two types of boundaries enhances the overall ductility of  $\text{Ni}_3\text{Al}$ .

## Conclusions

Thin foils of stoichiometric  $\text{Ni}_3\text{Al}$  below 100  $\mu\text{m}$  in thickness with crack free and smooth surfaces were fabricated by cold rolling without intermediate annealing. The basic mechanical properties of cold rolled—and heat treated—foils were examined and the following results were obtained:

1. Foils rolled over 80% reduction have strong  $\{110\}$  textures with various rolling directions depending on the initial orientations. The deformation microstructure of the rolled foils consists of fine slip lines and coarse and wavy shear band. Some of the foils, sample No. 31-2 and 47-1, shows banded structure. The Vickers hardness numbers of the foils cold rolled to 83% are extremely high: 604 and 649 for sample Nos. 42-2 and 47-1, respectively. These foils show high ultimate tensile strength of 1.7 GPa for sample No. 42-2 and 1.9 GPa for sample No. 47-1. The foils show no tensile ductility but they can be bent. There is no significant difference in the mechanical properties between the foils which have different rolling directions and deformation microstructure from each other.

2. The foils recrystallized at 1273 K and 1573 K for 1.8 ks had some ductility, 3 to 14.6%, in contrast to cast, polycrystalline  $\text{Ni}_3\text{Al}$ , which normally shows almost no elongation. The ductility was mainly related to the area fraction of low angle and  $\Sigma 3$  coincidence site lattice boundaries, which ranged from 41 to 84% depending on the heat treatment temperature. These boundaries are considered to be more crack-resistant than other boundaries, i.e. high  $\Sigma$  and random types.

## Acknowledgment

This research was supported partially by the Division of Materials Science and Engineering at the Oak Ridge National Laboratory, managed by UT-Battelle, LLC, for the U.S. Department of Energy under contract DE-AC05-00OR22725.

## References

- [1] Spearing, S. M., "Materials Issues in Microelectromechanical Systems (MEMS)," *Acta Materialia*, Vol. 48, 2000, pp. 179–196.
- [2] Theiss, S. D., Wu, C. C., Lu, M., Sturm, J. C., and Wagner, S., "Flexible, Lightweight Steel-Foil Substrates for a Si:H Thin-Film Transistor," *Material Research Society Symposium Proceedings*, Vol. 471, 1997, pp. 21–26.
- [3] Suo, Z., Ma, E. Y., Gleskova, H., and Wagner, S., "Mechanics of Rollable and Foldable Film-on-Foil Electronics," *Applied Physics Letters*, Vol. 74, 1999, pp. 1177–1179.
- [4] Ma, E. Y. and Wagner, S., "Amorphous Silicon Transistors on Ultrathin Steel Foil Substrates," *Applied Physics Letters*, Vol. 74, 1999, pp. 2661–2662.
- [5] Brandes, E. A. and Brook, G. B., Eds., *Smithells Metals Reference Book*, 7th ed., 1992.
- [6] Golberg, D., Demura, M., and Hirano, T., "Effect of Al-Rich Off-Stoichiometry on the Yield Stress of Binary Ni<sub>3</sub>Al Single Crystals," *Acta Materialia*, Vol. 46, 1998, pp. 2695–2703.
- [7] Stoloff, N. S., "Physical and Mechanical Metallurgy of Ni<sub>3</sub>Al and Its Alloys," *International Materials Reviews*, Vol. 34, 1989, pp. 153–183.
- [8] Epstein, A. H. and Senturia, S. D., "Macro Power from Micro Machinery," *Science*, Vol. 276, 1997, p. 1211.
- [9] Aoki, K. and Izumi, O., "On the Ductility of the Intermetallic Compound Ni<sub>3</sub>Al," *Transactions JIM (the Japan Institute of Metals)*, Vol. 19, 1978, pp. 203–210.
- [10] Aoki, K. and Izumi, O., "Improvement in Room Temperature Ductility of the L1<sub>2</sub> Type Intermetallic Compound Ni<sub>3</sub>Al by Boron Addition," *Nihon Kinzoku Gakkai Shi*, Vol. 43, 1979, pp. 1190–1196.
- [11] Liu, C. T., White, C. L., and Horton, J. A., "Effect of Boron on Grain-Boundaries in Ni<sub>3</sub>Al," *Acta Metallurgica*, Vol. 33, 1985, pp. 213–229.
- [12] Liu, C. T. and Sikka, V. K., "Nickel Aluminides for Structural Use," *Journal of Metals*, Vol. 38, 1986, pp. 19–21.
- [13] Hirano, T., "Improvement of Room Temperature Ductility of Stoichiometric Ni<sub>3</sub>Al by Unidirectional Solidification," *Acta Metallurgica et Materialia*, Vol. 38, 1990, pp. 2667–2671.
- [14] Hirano, T., "Tensile Ductility of Stoichiometric Ni<sub>3</sub>Al Grown by Unidirectional Solidification," *Scripta Metallurgica et Materialia*, Vol. 25, 1991, pp. 1747–1750.
- [15] Hirano, T. and Kainuma, T., "Improvement of Room-Temperature Ductility of Stoichiometric Ni<sub>3</sub>Al by Unidirectional Solidification," *ISIJ (The Iron and Steel Institute of Japan) International*, Vol. 31, 1991, pp. 1134–1138.
- [16] Watanabe, T., Hirano, T., Ochiai, T., Oikawa, H., "Texture and Grain Boundary Character Distribution (GBCD) in b-Free Ductile Polycrystalline Ni<sub>3</sub>Al," *Materials Science Forum*, Vol. 157-162, 1994, pp. 1103–1108.
- [17] Demura, M. and Hirano T., "Stress Response by the Strain-Rate Change in a Binary Stoichiometric Ni<sub>3</sub>Al Single Crystal," *Philosophical Magazine Letter*, Vol. 75, 1997, pp. 143–148.
- [18] Golberg, D., Demura M., and Hirano, T., "Single Crystal Growth and

- Characterization of Binary Stoichiometric and Al-rich Ni<sub>3</sub>Al,” *Journal of Crystal Growth*, Vol. 186, 1998, pp. 624–628.
- [19] Demura M., Suga, Y., Umezawa, O., Kishida, K., George, E. P., and Hirano, T., “Fabrication of Ni<sub>3</sub>Al Thin Foil by Cold Rolling,” unpublished work, 2000.
- [20] George E. P., Liu, C. T., and Pope, D. P., “Environmental Embrittlement: the Major Cause of Room-Temperature Brittleness in Polycrystalline Ni<sub>3</sub>Al,” *Scripta Metallurgica et Materialia*, Vol. 27, 1992, pp. 365–370.
- [21] George E. P., Liu, C. T., and Pope, D. P., “Intrinsic Ductility and Environmental Embrittlement of Binary Ni<sub>3</sub>Al,” *Scripta Metallurgica et Materialia*, Vol. 28, 1993, pp. 857–862.
- [22] Brandon, D. G., “The Structure of High-Angle Grain Boundaries,” *Acta Metallurgica*, Vol. 14, 1966, pp. 1479–1484.
- [23] Ball, J. and Gottstein, G., “Large Train Deformation of Ni<sub>3</sub>Al + B: Part I. Microstructure and Texture Evolution During Rolling,” *Intermetallics*, 1993, Vol. 1, pp. 171–185.
- [24] Gottstein, G., Nagpal, P., and Kim, W., “Recrystallization and Texture in Boron-Doped Ni<sub>3</sub>Al,” *Materials Science and Engineering A*, Vol. 108, 1989, pp. 165–179.
- [25] Hanada, S., Ogura, T., Watanabe, S., Izumi, O., and Masumoto, T., “Application of the Selected Area Channeling Pattern Method to the Study of Intergranular Fracture in Ni<sub>3</sub>Al,” *Acta Metallurgica*, Vol. 34, 1986, pp. 13–21.
- [26] Lin, H. and Pope, D. P., “The Influence of Grain-Boundary Geometry on Intergranular Crack-Propagation in Ni<sub>3</sub>Al,” *Acta Metallurgica et Materialia*, Vol. 41, 1993, pp. 553–562.
- [27] Su, J. Q., Demura, M., and Hirano, T., “Grain Boundary Fracture Strength in Ni<sub>3</sub>Al Bicrystals,” unpublished work, 2000.